Line-of-Sight Curved Path Following for Underactuated USVs and AUVs in the Horizontal Plane under the influence of Ocean Currents

Signe Moe[1], Kristin Y. Pettersen[1], Thor I. Fossen[1] and Jan T. Gravdahl[2]

***Abstract*— An essential ability of autonomous unmanned surface vessels (USVs) and autonomous underwater vehicles (AUVs) moving in a horizontal plane is to follow a general two-dimensional path in the presence of unknown ocean currents. This paper presents a method to achieve this. The proposed guidance and control system only requires absolute velocity measurements for feedback, thereby foregoing the need for expensive sensors to measure relative velocities. The closed-loop system consists of a guidance law and an adaptive feedback linearizing controller combined with sliding mode, and is shown to render the path cross-track error dynamics UGAS and USGES. Simulation results are presented to verify the theoretical results.**

I. INTRODUCTION

The use of unmanned marine vehicles is rapidly increasing within several fields, such as marine biology, environmental monitoring, seafloor mapping, oceanography, military use and in the oil and gas industry. Therefore, control of such autonomous vessels is considered an important area within the marine control research community. This paper addresses a cornerstone ability for an underactuated USV, namely path following of a general path in the presence of unknown ocean currents. Note that the results presented in this paper are also applicable to an AUV moving in the horizontal plane. Path following is a motion control scenario where the controlled vessel has to follow a predefined path without time constraints [1]-[3]. In this paper, the vessel should converge to and follow a certain path while fulfilling a velocity assignment. Thus, it may be considered a maneuvering control problem [4] with a geometric and a dynamic task.

A commonly used approach for path following and maneuvering control is the Line of Sight (LOS) method [1],[5]-[10]. LOS is a guidance method providing a heading reference to the USV that, if satisfied, will ensure convergence to the desired path. However, this control approach is susceptible to environmental disturbances such as ocean currents, waves and wind: path deviation and convergence problems will occur if the vessel is affected by environmental disturbances [11]. For straight line paths, LOS can be used with integral action [11]-[13] or adaptive estimation techniques [7] by allowing the USV to side-slip to compensate for the effect of the ocean current. In [12] the steady state of the marine vessel is used to estimate the ocean current magnitude and direction, and in [7] the estimates of the ocean current is used directly in the LOS guidance law.

For curved path following, the USV has to sideslip even without ocean currents to achieve path following due to the non-zero curvature of the path. Rigorous stability properties for LOS with side-slip used on a general, curved path when ocean current is not considered is given in [14]. The side-slip is calculated based on velocity measurements. A similar approach is used in [15], where path following of general paths for both surface and underwater vehicles is achieved by analyzing Serret-Frenet equations.

Side-slipping is required both for curved path following and for ocean current compensation, and thus also in the case when these two scenarios are combined. In [16], a LOS path following approach is used with current estimation techniques and measurements of relative velocities, allowing the USV to follow curved paths while compensating for the influence of ocean currents. The Serret-Frenet based method in [15] is extended to account for the effects of ocean current for surface and underwater vehicles in [17] and [18], respectively. Similar to [16], this method requires estimation of the ocean current, measurements of relative velocities and a parametrization of the path as a function of arc length, which can make it challenging to find a parametrization of the desired path. Furthermore, for the underwater case, it is also required that the path torsion and curvature is known as functions of arc length.

This paper proves that the LOS guidance law suggested in [14] for curved path following is suitable also for curved path following in combination with ocean current compensation by using adaptive feedback linearization combined with sliding mode. The proposed guidance and control system requires measurements of absolute velocities only, thereby foregoing the need for expensive sensors to measure relative velocities. Furthermore, the guidance law is not based on Serret-Frenet frames, which allows for any parametrization of the path and removes the need for an update law for the Serret-Frenet frame.

This paper is organized as follows. Section II presents the USV model before the control objectives are formalized in Section III. The suggested control system is then introduced in Section IV followed by the main result in Section V. Finally, simulations results and conclusions are presented in Sections VI and VII, respectively.

[1]S.Moe, K.Y.Pettersen and T.I. Fossen are with the NTNU Center for Autonomous Marine Operations and Systems (AMOS), at The Department of Engineering Cybernetics, Norwegian University of Science and Technology (NTNU), Trondheim, Norway {signe.moe, kristin.y.pettersen, thor.fossen}@ntnu.no

[2]J.T. Gravdahl is with The Department of Engineering Cybernetics, Norwegian University of Science and Technology (NTNU), Trondheim, Norway jan.tommy.gravdahl@itk.ntnu.no

II. VESSEL MODEL

This section presents the 3-DOF surface vessel maneuvering model that is considered and the assumptions on which this is based.

A. Model Assumptions

Assumption 1. The motion of the USV is described by 3 degrees of freedom (DOF), that is surge, sway and yaw.
Assumption 2. The USV is port-starboard symmetric.
Assumption 3. The body-fixed coordinate frame b is located at a distance $(x_g^\star, 0)$ from the USV's center of gravity (CG) along the center-line of the USV, where $x_g^\star$ is to be defined later.
Remark 1. The body-fixed coordinate system can always be translated to the required location $x_g^\star$ [1].
Assumption 4. The ocean current in the inertial frame i $\boldsymbol{V}_c \triangleq [V_x, V_y, 0]^T$ is constant, irrotational and bounded. Hence there exists a constant $V_{\max} > 0$ such that $V_{\max} > \sqrt{V_x^2 + V_y^2}$.

B. The Vessel Model

The state of the surface vessel is given by the vector $\boldsymbol{\eta} \triangleq [x, y, \psi]^T$ and describes the position (x, y) and the orientation ψ of the USV with respect to the inertial frame i. The vector $\boldsymbol{\nu} \triangleq [u, v, r]^T$ contains the linear and angular velocities of the USV defined in the body-fixed frame b, where u is the surge velocity, v is the sway velocity and r is the yaw rate. The ocean current velocity in the body frame b, $\boldsymbol{\nu}_c \triangleq [u_c, v_c, 0]^T$, is obtained from $\boldsymbol{\nu}_c = \boldsymbol{R}^T(\psi)[V_x, V_y, 0]^T$, where $\boldsymbol{R}(\psi)$ is defined as

$$\boldsymbol{R}(\psi) \triangleq \begin{bmatrix} \cos(\psi) & -\sin(\psi) & 0 \\ \sin(\psi) & \cos(\psi) & 0 \\ 0 & 0 & 1 \end{bmatrix}. \tag{1}$$

The relative velocity

$$\boldsymbol{\nu}_r = \begin{bmatrix} u_r \\ v_r \\ r \end{bmatrix} \triangleq \boldsymbol{\nu} - \boldsymbol{\nu}_c = \begin{bmatrix} u \\ v \\ r \end{bmatrix} - \begin{bmatrix} u_c \\ v_c \\ 0 \end{bmatrix} \tag{2}$$

is defined in the body frame b.

The following 3-DOF maneuvering model is considered [1], [11]:

$$\begin{aligned} \dot{\boldsymbol{\eta}} &= \boldsymbol{R}(\psi)\boldsymbol{\nu} \\ \boldsymbol{M}_{RB}\dot{\boldsymbol{\nu}} + \boldsymbol{C}_{RB}(\boldsymbol{\nu})\boldsymbol{\nu} &= -\boldsymbol{M}_A\dot{\boldsymbol{\nu}}_r - \boldsymbol{C}_A(\boldsymbol{\nu}_r)\boldsymbol{\nu}_r - \boldsymbol{D}(\boldsymbol{\nu}_r)\boldsymbol{\nu}_r + \boldsymbol{B}\boldsymbol{f} \end{aligned} \tag{3}$$

The vector $\boldsymbol{f} \triangleq [T, \delta]^T$ contains the control inputs: T is the thruster force and δ is the rudder angle. The matrix $\boldsymbol{M}_{RB} = \boldsymbol{M}_{RB}^T > 0$ is the rigid-body mass and inertia matrix and $\boldsymbol{C}_{RB}$ is the rigid-body Coriolis and centripetal matrix. Similarly, $\boldsymbol{M}_A = \boldsymbol{M}_A^T > 0$ and $\boldsymbol{C}_A$ are mass and Coriolis matrices for hydrodynamic added mass. The strictly positive hydrodynamic matrix is given by $\boldsymbol{D}$ and $\boldsymbol{B} \in \mathbb{R}^{3\times 2}$ is the actuator configuration matrix. The matrices have the following structure:

$$\begin{aligned} &\boldsymbol{M}_x \triangleq \begin{bmatrix} m_{11}^x & 0 & 0 \\ 0 & m_{22}^x & m_{23}^x \\ 0 & m_{23}^x & m_{33}^x \end{bmatrix}, \ \boldsymbol{D}(\boldsymbol{\nu}_r) \triangleq \begin{bmatrix} d_{11} + d_{11}^q u_r & 0 & 0 \\ 0 & d_{22} & d_{23} \\ 0 & d_{32} & d_{33} \end{bmatrix}, \\ &\boldsymbol{B} \triangleq \begin{bmatrix} b_{11} & 0 \\ 0 & b_{22} \\ 0 & b_{32} \end{bmatrix}, \ \boldsymbol{C}_x(\boldsymbol{z}) \triangleq \begin{bmatrix} 0 & 0 & -m_{22}^x z_2 - m_{23}^x z_3 \\ 0 & 0 & m_{11}^x z_1 \\ m_{22}^x z_2 + m_{23}^x z_3 & -m_{11}^x z_1 & 0 \end{bmatrix}, \end{aligned} \tag{4}$$

for $x \in \{RB, A\}$. Assumptions 1-3 justify the structure of the matrices $\boldsymbol{M}_x$, $x \in \{RB, A\}$, and $\boldsymbol{D}$ and the structure of $\boldsymbol{C}$ is obtained as described in [1]. Furthermore, the distance $x_g^\star$ from Assumption 3 is chosen so that $\boldsymbol{M}^{-1}\boldsymbol{B}\boldsymbol{f} = [\tau_u, 0, \tau_r]^T$. This point $(x_g^\star, 0)$ exists for all port-starboard symmetric ships [11]. Here, $\boldsymbol{M} = \boldsymbol{M}_{RB} + \boldsymbol{M}_A$.
Remark 2. Note that the model (3) does not depend on wave frequency. Hence, the parameters in $\boldsymbol{M}_A$ and $\boldsymbol{D}$ can be considered constant.
Remark 3. It is shown in [1] that since the ocean current is constant and irrotational in i, the USV can be described by the 3-DOF maneuvering model in (3).
Remark 4. The above model is valid for ships with a non-negative relative surge velocity u_r, implying that the ship is not moving backwards relative to the ocean current. This is a valid assumption for a ship with a path-following task.

C. The Model in Component Form

For the control design it is useful to expand (3) into component form:

$$\begin{aligned} \dot{x} &= \cos(\psi)u - \sin(\psi)v \\ \dot{y} &= \sin(\psi)u + \cos(\psi)v \\ \dot{\psi} &= r, \\ \dot{u} &= -\frac{d_{11} + d_{11}^q u}{m_{11}}u + \frac{(m_{22}v + m_{23}r)r}{m_{11}} + \boldsymbol{\phi}_u^T(\psi, r)\boldsymbol{\theta}_u + \boldsymbol{\tau}_u \\ \dot{v} &= X(u_r, u_c)r + Y(u_r)v_r \\ \dot{r} &= F_r(u, v, r) + \boldsymbol{\phi}_r^T(u, v, r, \psi)\boldsymbol{\theta}_r + \tau_r \end{aligned} \tag{5}$$

Here, $m_{ij} \triangleq m_{ij}^{RB} + m_{ij}^A$ and $\boldsymbol{\theta}_u = \boldsymbol{\theta}_r = [V_x, V_y, V_x^2, V_y^2, V_x V_y]^T$. The expressions for $\boldsymbol{\phi}_u^T(\psi, r)$, $X(u_r, u_c)$, $Y(u_r)$, $F_r(u, v, r)$ and $\boldsymbol{\phi}_r^T(u, v, r, \psi)$ are given in Appendix A.

III. CONTROL OBJECTIVES

This section formalizes the control problem solved in this paper: The control system should make the vessel follow a given smooth path C and maintain a desired constant surge velocity u_{des} in the presence of unknown constant irrotational ocean currents. C is parametrized with respect to the inertial frame i. Let $\theta \geq 0$ denote the path variable. Then, the path C is parametrized by $(x_p(\theta), y_p(\theta))$.

The cross-track error y_e is computed as the orthogonal distance between the vessel position (x, y) to the path-tangential reference frame defined by the point $(x_p(\theta), y_p(\theta))$. The path variables are illustrated in Fig. 1. Note that the position of the

path-tangential reference frame is always such that the along-track error $x_e = 0$. The path-tangential frame corresponds to the inertial frame rotated by $\gamma_p(\theta)$, where

$$\gamma_p(\theta) = \text{atan}\left(\frac{y_p'(\theta)}{x_p'(\theta)}\right). \tag{6}$$

Hence,

$$\begin{bmatrix} 0 \\ y_e \end{bmatrix} = \boldsymbol{R}^T(\gamma_p(\theta)) \begin{bmatrix} x - x_p(\theta) \\ y - y_p(\theta) \end{bmatrix} \tag{7}$$

where $\boldsymbol{R}$ is the rotation matrix defined in (1). Thus, the cross-track error is given as

$$y_e = -(x - x_p(\theta))\sin(\gamma_p(\theta)) + (y - y_p(\theta))\cos(\gamma_p(\theta)), \tag{8}$$

where the propagation of θ is given by [1]:

$$\dot{\theta} = \frac{U}{\sqrt{x_p'(\theta)^2 + y_p'(\theta)^2}} > 0, \tag{9}$$

and

$$U = \sqrt{u^2 + v^2}. \tag{10}$$

Note that it is assumed that the path is an open curve, i.e. the end point is different from the start point. Definition [14] guarantees that there is a unique solution for the cross-track error y_e obtained by minimizing θ.

It can be shown that the cross-track error dynamics can be expressed as [14]

$$\begin{aligned} \dot{y}_e = &-(u\cos(\psi) - v\sin(\psi))\sin(\gamma_p(\theta)) \\ &+ (u\sin(\psi) + v\cos(\psi))\cos(\gamma_p(\theta)). \end{aligned} \tag{11}$$

It is obvious from Fig. 1 that $y_e = 0$ implies that the vessel is on the desired path. Hence, we define the control objectives as

$$\begin{aligned} \lim_{t\to\infty} u(t) &= u_{\text{des}} \\ \lim_{t\to\infty} y_e(t) &= 0 \end{aligned} \tag{12}$$

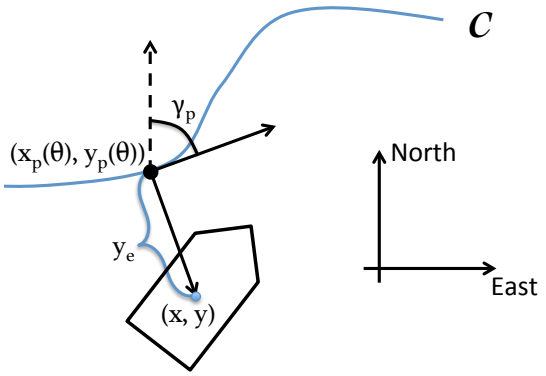

Fig. 1: Desired path C, path-tangential reference frame with orientation $\gamma_p(\theta)$ and cross-track error y_e illustrated.

IV. THE CONTROL SYSTEM

This Section presents the proposed guidance law and controllers. The system uses absolute velocity measurements only, making it unnecessary to buy expensive sensors to measure relative velocities. The reason why only absolute velocity measurements are required, is that the absolute velocity is the sum of relative velocity and ocean currents, and thus implicitly contains information about these two components although the exact composition of relative velocities and ocean currents are unknown. Thus, by the design of the control system. the vessel is able to compensate both for the curvature of the path and the ocean current without knowing the exact components of these measurements.

A. Guidance Laws

The desired surge velocity is chosen to be constant and positive.

$$u_{\text{des}}(t) > 0 \tag{13}$$

The guidance law for the USV heading is chosen as

$$\psi_{\text{des}} = \gamma_p(\theta) - \underbrace{\text{atan}\left(\frac{v}{u_{\text{des}}}\right)}_{\triangleq \beta_{\text{des}}} - \text{atan}\left(\frac{y_e}{\Delta}\right). \tag{14}$$

B. Surge and Yaw Controllers

We define the following error signals:

$$\tilde{u} = u - u_{\text{des}} \tag{15}$$

$$\tilde{\psi} = \psi - \psi_{\text{des}} \tag{16}$$

$$\dot{\tilde{\psi}} = r - \dot{\psi}_{\text{des}} \tag{17}$$

$$\boldsymbol{\xi} = \begin{bmatrix} \tilde{u} & \tilde{\psi} & \dot{\tilde{\psi}} \end{bmatrix}^T \tag{18}$$

An adaptive feedback linearizing PD-controller is used to ensure tracking of the desired heading ψ_{des}:

$$\begin{aligned} \tau_r = &-F_r(u,v,r) - \boldsymbol{\phi}_r^T(u,v,r,\psi)\hat{\boldsymbol{\theta}}_r + \ddot{\psi}_{\text{des}} \\ &- (k_\psi + \lambda k_r)\tilde{\psi} - (k_r + \lambda)\dot{\tilde{\psi}} - k_d \text{sign}(\dot{\tilde{\psi}} + \lambda\tilde{\psi}) \end{aligned} \tag{19}$$

$$\dot{\hat{\boldsymbol{\theta}}}_r = \gamma_r \boldsymbol{\phi}_r(u,v,r,\psi)\left(\dot{\tilde{\psi}} + \lambda\tilde{\psi}\right) \tag{20}$$

The gains $k_\psi, k_r, \lambda, \gamma_r > 0$ are constant and positive, and the function $\text{sign}(x)$ returns 1, 0 and -1 when x is positive, zero or negative, respectively.

An adaptive feedback linearizing P-controller is used to ensure tracking of the desired surge velocity u_{des}:

$$\begin{aligned} \tau_u = &-\frac{1}{m_{11}}(m_{22}v + m_{23}r)r + \frac{d_{11}}{m_{11}}u_{\text{des}} - \boldsymbol{\phi}_u^T(\psi,r)\hat{\boldsymbol{\theta}}_u \\ &+ \frac{d_{11}^q}{m_{11}}u^2 + \dot{u}_{\text{des}} - k_u\tilde{u} - k_e \text{sign}(\tilde{u}) \end{aligned} \tag{21}$$

$$\dot{\hat{\boldsymbol{\theta}}}_u = \gamma_u \boldsymbol{\phi}_u(\psi,r)\tilde{u} \tag{22}$$

The gains k_u, k_e, γ_u are strictly positive constant controller gains.

The proposed controllers are similar to the controllers in [11], but in this paper the terms $k_d \text{sign}(\dot{\tilde{\psi}} + \lambda\tilde{\psi})$ and

$k_e \text{sign}(\tilde{u})$ have been added to increase the robustness of the controller with respect to model uncertainties. Note that the controllers (19) and (21) rely only on absolute velocity measurements, as relative velocities are not available for feedback.

Proposition 1. *Given an underactuated surface vessel described by the dynamical system (5). If Assumptions 1-4 hold, the adaptive controllers (19)-(20) and (21)-(22) ensure that* $\boldsymbol{\xi} = \mathbf{0}$ *is a uniformly globally exponentially stable (UGES) equilibrium point and that the references provided by the guidance system are exponentially tracked.*

Proof. Defining

$$\tilde{\boldsymbol{\theta}}_r = \hat{\boldsymbol{\theta}}_r - \boldsymbol{\theta}_r, \tag{23}$$

$$s = \dot{\tilde{\psi}} + \lambda \tilde{\psi}, \tag{24}$$

the error dynamics of the heading controller system can be expressed as

$$\begin{bmatrix} \dot{\tilde{\psi}} \\ \dot{s} \end{bmatrix} = \begin{bmatrix} -\lambda & 1 \\ -k_\psi & -k_r \end{bmatrix} \begin{bmatrix} \tilde{\psi} \\ s \end{bmatrix} - \begin{bmatrix} \mathbf{0} \\ \boldsymbol{\phi}_r^T \end{bmatrix} \tilde{\boldsymbol{\theta}}_r - \begin{bmatrix} 0 \\ k_d \text{sign}(s) \end{bmatrix} \tag{25}$$

$$\dot{\tilde{\boldsymbol{\theta}}}_r = \gamma_r \boldsymbol{\phi}_r(u, v, r, \psi) s \tag{26}$$

To analyze the stability properties of the interconnected system (25)-(26), we consider the positive definite and radially unbounded Lyapunov function candidate

$$V = \frac{1}{2} k_\psi \tilde{\psi}^2 + \frac{1}{2} s^2 + \frac{1}{2\gamma_r} \tilde{\boldsymbol{\theta}}_r^T \tilde{\boldsymbol{\theta}}_r \tag{27}$$

$$\Downarrow$$

$$\dot{V} = -\lambda k_\psi \tilde{\psi}^2 - k_r s^2 - k_d |s| \leq 0. \tag{28}$$

$\dot{V}$ is negative semi-definite, and thus the origin $(\tilde{\psi}, s, \tilde{\boldsymbol{\theta}}_r) = (0, 0, \mathbf{0})$ is a uniformly globally stable (UGS) equilibrium point of the interconnected system (25)-(26) [19]. Since $V(t) \leq V(0)$, $\tilde{\psi}$, s and $\tilde{\boldsymbol{\theta}}_r$ are bounded. Thus, there exists some bounds α, β, ζ such that

$$|\tilde{\psi}(t)| \leq \alpha \tag{29}$$

$$|s(t)| \leq \beta \qquad \forall\ t \geq 0 \tag{30}$$

$$||\tilde{\boldsymbol{\theta}}_r(t)|| \leq \zeta \tag{31}$$

It is straightforward to show that

$$|\tilde{V}_x| \leq \sqrt{\tilde{V}_x^2 + \tilde{V}_y^2 + \tilde{V_x^2}^2 + \tilde{V_y^2}^2 + V_x \tilde{V_y}^2} = ||\tilde{\boldsymbol{\theta}}_r(t)|| < \zeta \tag{32}$$

$$|\tilde{V}_y| \leq ||\tilde{\boldsymbol{\theta}}_r(t)|| < \zeta \tag{33}$$

$$\vdots$$

$$|V_x \tilde{V}_y| \leq ||\tilde{\boldsymbol{\theta}}_r(t)|| < \zeta \tag{34}$$

Thus,

$$\begin{aligned} |\boldsymbol{\phi}_r^T \tilde{\boldsymbol{\theta}}_r| &= |\phi_1 \tilde{V}_x + \phi_2 \tilde{V}_y + \phi_3 \tilde{V_x^2} + \phi_4 \tilde{V_y^2} + \phi_5 V_x \tilde{V}_y| \\ &\leq |\phi_1||\tilde{V}_x| + |\phi_2||\tilde{V}_y| + |\phi_3||\tilde{V_x^2}| + |\phi_4||\tilde{V_y^2}| + |\phi_5||V_x \tilde{V}_y| \\ &\leq \zeta\,(|\phi_1| + |\phi_2| + |\phi_3| + |\phi_4| + |\phi_5|) = \zeta |\boldsymbol{\phi}_r| \end{aligned} \tag{35}$$

Since the equilibrium point $(\tilde{\psi}, s, \tilde{\boldsymbol{\theta}}_r) = (0, 0, \mathbf{0})$ is UGS, the states have no finite escape time and the system (25)-(26) is forward complete. Thus, we can analyze (25) under the assumption that $\tilde{\boldsymbol{\theta}}_r$ is a bounded time-varying signal. Consider the positive definite and radially unbounded Lyapunov function candidate

$$V_\psi = \frac{1}{2} k_\psi \tilde{\psi}^2 + \frac{1}{2} s^2 \tag{36}$$

$$\Downarrow$$

$$\begin{aligned} \dot{V}_\psi &= -\lambda k_\psi \tilde{\psi}^2 - k_r s^2 - \boldsymbol{\phi}_r^T \tilde{\boldsymbol{\theta}} s - k_d |s| \\ &\leq -\lambda k_\psi \tilde{\psi}^2 - k_r s^2 + (|\boldsymbol{\phi}_r^T \tilde{\boldsymbol{\theta}}| - k_d)|s| \\ &\leq -\lambda k_\psi \tilde{\psi}^2 - k_r s^2 + (\zeta |\boldsymbol{\phi}_r| - k_d)|s| \end{aligned} \tag{37}$$

We choose the gain $k_d > 2\zeta |\boldsymbol{\phi}_r|$. Thus,

$$\begin{aligned} \dot{V}_\psi &\leq -\lambda k_\psi \tilde{\psi}^2 - k_r s^2 - \zeta |\boldsymbol{\phi}_r||s| \\ &\leq -\lambda k_\psi \tilde{\psi}^2 - k_r s^2 < 0. \end{aligned} \tag{38}$$

$\dot{V}_\psi$ is negative definite, and thus the origin $(\tilde{\psi}, s) = (0, 0)$ is a uniformly asymptotically globally stable (UGAS) equilibrium point of the system (25). Furthermore, Theorem 4.10 [20] is satisfied with $k_1 = \min(k_\psi/2, 1/2)$, $k_2 = \max(k_\psi/2, 1/2)$, $k_3 = \min(\lambda k_\psi, k_r)$ and $a = 2$. This implies that the origin $(\tilde{\psi}, s) = (0, 0)$ is a uniformly exponentially globally stable (UGES) equilibrium point of the system (25), and

$$\lim_{t \to \infty} \tilde{\psi} = 0, \tag{39}$$

$$\lim_{t \to \infty} \dot{\tilde{\psi}} = \lim_{t \to \infty} s - \lambda \tilde{\psi} = 0. \tag{40}$$

Similarly, defining

$$\tilde{\boldsymbol{\theta}}_u = \hat{\boldsymbol{\theta}}_u - \boldsymbol{\theta}_u, \tag{41}$$

the error dynamics of the surge controller system is given by

$$\dot{\tilde{u}} = -\left(\frac{d_{11}}{m_{11}} + k_u \right) \tilde{u} - \boldsymbol{\phi}_u^T(\psi, r) \tilde{\boldsymbol{\theta}}_u - k_e \text{sign}(\tilde{u}) \tag{42}$$

$$\dot{\tilde{\boldsymbol{\theta}}}_u = \gamma_u \boldsymbol{\phi}_y(\psi, r) \tilde{u} \tag{43}$$

To analyze the stability properties of the interconnected system (42)-(43), we consider the positive definite and radially unbounded Lyapunov function candidate

$$V = \frac{1}{2} \tilde{u}^2 + \frac{1}{2\gamma_u} \tilde{\boldsymbol{\theta}}_u^T \tilde{\boldsymbol{\theta}}_u \tag{44}$$

$$\Downarrow$$

$$\dot{V} = -\left(\frac{d_{11}}{m_{11}} + k_u \right) \tilde{u}^2 - k_e |\tilde{u}| \leq 0. \tag{45}$$

$\dot{V}$ is negative semi-definite, and thus the origin $(\tilde{u}, \tilde{\boldsymbol{\theta}}_u) = (0, \mathbf{0})$ is an UGS equilibrium point of the interconnected system (42)-(43). Since $V(t) \leq V(0)$, $\tilde{u}$, and $\tilde{\boldsymbol{\theta}}_u$ are bounded. Thus, there exists some bounds α, β, ζ such that

$$|\tilde{u}(t)| \leq \iota \qquad \forall\ t \geq 0 \tag{46}$$

$$||\tilde{\boldsymbol{\theta}}_u(t)|| \leq \kappa \tag{47}$$

Similarly as the analysis for system (25), we can analyze (42) under the assumption that $\tilde{\boldsymbol{\theta}}_u$ is a bounded time-varying

signal. Consider the positive definite and radially unbounded Lyapunov function candidate

$$V_u = \frac{1}{2}\tilde{u}^2 \tag{48}$$
$$\Downarrow$$
$$\begin{aligned}\dot{V}_u &= -\left(\frac{d_{11}}{m_{11}}+k_u\right)\tilde{u}^2 - \boldsymbol{\phi}_t^T\tilde{\boldsymbol{\theta}}_u\tilde{u} - k_e|\tilde{u}| \\ &\leq -\left(\frac{d_{11}}{m_{11}}+k_u\right)\tilde{u}^2 + (|\boldsymbol{\phi}_t^T\tilde{\boldsymbol{\theta}}_u| - k_e)|\tilde{u}| \\ &\leq -\left(\frac{d_{11}}{m_{11}}+k_u\right)\tilde{u}^2 + (\kappa|\boldsymbol{\phi}_t| - k_e)|\tilde{u}| \end{aligned} \tag{49}$$

We choose the gain $k_e > 2\kappa|\boldsymbol{\phi}_u|$. Thus,

$$\begin{aligned}\dot{V}_\psi &\leq -\left(\frac{d_{11}}{m_{11}}+k_u\right)\tilde{u}^2 - \kappa|\boldsymbol{\phi}_t||\tilde{u}| \\ &\leq -\left(\frac{d_{11}}{m_{11}}+k_u\right)\tilde{u}^2 < 0. \end{aligned} \tag{50}$$

$\dot{V}_u$ is negative definite, and thus the origin $\tilde{u}0$ is a uniformly asymptotically globally stable (UGAS) equilibrium point of the system (42). Furthermore, Theorem 4.10 [20] is satisfied with $k_1 = k_2 = 1/2$, $k_3 = d_{11}/m_{11} + k_u$ and $a = 2$. This implies that the origin $\tilde{u} = 0$ is a uniformly exponentially globally stable (UGES) equilibrium point of the system (42), and

$$\lim_{t\to\infty}\tilde{u} = 0. \tag{51}$$

Thus, the errors $\boldsymbol{\xi} = \begin{bmatrix}\tilde{u} & \tilde{\psi} & \dot{\tilde{\psi}}\end{bmatrix}^T$ converge exponentially to zero. □

Assumption 5. The controllers (19) and (21) are tuned such that the error dynamics in (25) and (42) is fast compared to the cross-track error dynamics (11). Hence, $\boldsymbol{\xi}$ can be assumed to be zero.

C. State Measurements

The control system proposed in this paper assumes that $\boldsymbol{\eta}$ and $\boldsymbol{\nu}$ are measured. Ships are usually equipped with a large variety of sensors that combined provide sensor data to estimate the vessel state [1]. We assume that the ship is equipped with Global Navigation Satellite System (GNSS) receivers to provide position and velocity measurements and a gyrocompass to measure yaw ψ yaw rate r. Furthermore, we assume that the measurements are filtered to remove first-order wave-induced motions and measurement noise.

V. MAIN RESULT

This section presents the conditions under which the proposed control system achieves the control objectives (12).

Theorem 1. *Given an underactuated surface vessel described by the dynamical system (5). If Assumptions 1-5 hold, the controllers given by (19) and (21), and the guidance laws given by (13) and (14), give a cross-track error dynamics for which the equilibrium point $y_e = 0$ is uniformly globally asymptotically stable (UGAS) and uniformly semi-globally exponentially stable (USGES), and the control objectives (12) are achieved.*

Proof. The dynamics of the path cross track error is given in (11), and can be rewritten as follows:

$$\begin{aligned}\dot{y}_e &= -\left(u\cos(\psi) - v\sin(\psi)\right)\sin\left(\gamma_{\mathrm{p}}(\theta)\right) \\ &\quad + \left(u\sin(\psi) + v\cos(\psi)\right)\cos\left(\gamma_{\mathrm{p}}(\theta)\right) \\ &= u\left(\sin(\psi)\cos(\gamma_{\mathrm{p}}(\theta)) - \cos(\psi)\sin(\gamma_{\mathrm{p}}(\theta))\right) \\ &\quad + v\left(\cos(\psi)\sin(\gamma_{\mathrm{p}}(\theta)) + \sin(\psi)\cos(\gamma_{\mathrm{p}}(\theta))\right) \\ &= (u_{\mathrm{des}} + \tilde{u})\sin(\psi - \gamma_{\mathrm{p}}(\theta)) + v\cos(\psi - \gamma_{\mathrm{p}}(\theta)) \\ &= U_{\mathrm{des}}\sin\left(\psi - \gamma_{\mathrm{p}}(\theta) + \beta_{c,\mathrm{des}}\right) + \tilde{u}\sin(\psi - \gamma_{\mathrm{p}}(\theta)), \end{aligned} \tag{52}$$

where

$$U_{\mathrm{des}} = \sqrt{u_{\mathrm{des}}^2 + v^2}. \tag{53}$$

Inserting the expressions for the guidance law in yaw (14) and error signal (16), the sine terms in (52) can be rewritten as below:

$$\begin{aligned}\sin\left(\psi - \gamma_{\mathrm{p}}(\theta) + \beta_{\mathrm{des}}\right) &= \sin\left(\tilde{\psi} + \psi_{\mathrm{des}} - \gamma_{\mathrm{p}}(\theta) + \beta_{\mathrm{des}}\right) \\ &= \sin\left(\tilde{\psi} - \mathrm{atan}\left(\frac{\mathrm{y_e}}{\Delta}\right)\right) \\ &= \sin(\tilde{\psi})\cos\left(\mathrm{atan}\left(\frac{\mathrm{y_e}}{\Delta}\right)\right) - \cos(\tilde{\psi})\sin\left(\mathrm{atan}\left(\frac{\mathrm{y_e}}{\Delta}\right)\right) \\ &= -\sin\left(\mathrm{atan}\left(\frac{\mathrm{y_e}}{\Delta}\right)\right) + \sin(\tilde{\psi})\cos\left(\mathrm{atan}\left(\frac{\mathrm{y_e}}{\Delta}\right)\right) \\ &\quad - (\cos(\tilde{\psi}) - 1)\sin\left(\mathrm{atan}\left(\frac{\mathrm{y_e}}{\Delta}\right)\right) \\ &= -\frac{y_e}{\sqrt{\Delta^2 + y_e^2}} \\ &\quad + \sin(\tilde{\psi})\frac{\Delta}{\sqrt{\Delta^2 + y_e^2}} - (\cos(\tilde{\psi}) - 1)\frac{y_e}{\sqrt{\Delta^2 + y_e^2}} \end{aligned} \tag{54}$$

$$\begin{aligned}\sin\left(\psi - \gamma_{\mathrm{p}}(\theta)\right) &= \sin\left(\tilde{\psi} + \psi_{\mathrm{des}} - \gamma_{\mathrm{p}}(\theta)\right) \\ &= \sin\left(\tilde{\psi} - \beta_{\mathrm{des}} - \mathrm{atan}\left(\frac{\mathrm{y_e}}{\Delta}\right)\right) \\ &= \sin\left(\tilde{\psi} - \mathrm{atan}\left(\frac{\Delta \mathrm{v} + \mathrm{y_e u_{des}}}{\Delta \mathrm{u_{des}} - \mathrm{y_e v}}\right)\right) \end{aligned} \tag{55}$$

Inserting (54)-(55) into (52) yields

$$\begin{aligned}\dot{y}_e &= U_{\mathrm{des}}\left(-\frac{y_e}{\sqrt{\Delta^2 + y_e^2}} + \sin(\tilde{\psi})\frac{\Delta}{\sqrt{\Delta^2 + y_e^2}}\right. \\ &\quad \left. - (\cos(\tilde{\psi}) - 1)\frac{y_e}{\sqrt{\Delta^2 + y_e^2}}\right) + \tilde{u}\sin\left(\tilde{\psi} - \mathrm{atan}\left(\frac{\Delta \mathrm{v} + \mathrm{y_e u_{des}}}{\Delta \mathrm{u_{des}} - \mathrm{y_e v}}\right)\right) \\ &= f_1(t, y_e) + \boldsymbol{g}(t, y_e, \boldsymbol{\xi})\boldsymbol{\xi} \end{aligned} \tag{56}$$

with

$$f_1(t, y_e) = -U_{\mathrm{des}}\frac{y_e}{\sqrt{\Delta^2 + y_e^2}}, \tag{57}$$

$$\boldsymbol{g}(t, y_e, \tilde{\psi}) = \begin{bmatrix}\sin\left(\tilde{\psi} - \mathrm{atan}\left(\frac{\Delta \mathrm{v} + \mathrm{y_e u_{des}}}{\Delta \mathrm{u_{des}} - \mathrm{y_e v}}\right)\right) \\ U_{\mathrm{des}} g_1(t, y_e, \tilde{\psi}) \\ 0\end{bmatrix}^T \tag{58}$$

where

$$g_1(t,y_e,\tilde{\psi}) = \frac{\sin(\tilde{\psi})}{\tilde{\psi}}\frac{\Delta}{\sqrt{\Delta^2+y_e^2}} - \frac{\cos(\tilde{\psi})-1}{\tilde{\psi}}\frac{y_e}{\sqrt{\Delta^2+y_e^2}} \tag{59}$$

By Assumption 5, $\boldsymbol{\xi} = \mathbf{0}$, reducing the error dynamics to

$$\dot{y}_e = f_1(t,y_e) = -U_{\text{des}}\frac{y_e}{\sqrt{\Delta^2+y_e^2}} \tag{60}$$

Stability of the nominal system can be shown using the quadratic, positive definite, decrescent and radially unbounded Lyapunov function $V = \frac{1}{2}y_e^2$.

$$\dot{V} = y_e\dot{y}_e = -\frac{U_{\text{des}}}{\sqrt{\Delta^2+y_e^2}}y_e^2. \tag{61}$$

Since

$$U_{\text{des}} = \sqrt{u_{\text{des}}^2+v^2} \geq u_{\text{des}} > 0 \tag{62}$$

by (13), $\dot{V}$ is negative definite along the trajectories of the system (57), which is UGAS, and

$$|y_e(t)| \leq |y_e(t_0)| \ \forall\ t \geq t_0. \tag{63}$$

Furthermore, using the same approach as the proof in Appendix A in [14], we define

$$\phi(t,y_e) = \frac{U_{\text{des}}}{\sqrt{\Delta^2+y_e^2}} \tag{64}$$

For each $r > 0$ and $|y_e(t)| \leq r$, we have

$$\phi(t,y_e) \geq \frac{u_{\text{des}}}{\sqrt{\Delta^2+r^2}} \triangleq c(r). \tag{65}$$

Consequently,

$$\dot{V}(y,y_e) = -2\phi(t,y_e)V(t,y_e) \leq -2c(r)V(t,y_e) \quad \forall\ |y_e(t)| \leq r \tag{66}$$

Given (63), the above holds for all trajectories generated by the initial conditions $y_e(t_0)$. Therefore, the comparison lemma (Lemma 3.4 [20]) can be used to prove that the equilibrium point $y_e = 0$ is USGES. The differential equation $\dot{z} = -2c(r)z$ has the solution $z(t) = e^{-2c(r)(t-t_0)}z(t_0)$, which implies that

$$w(t) \leq e^{-2c(r)(t-t_0)}w(t_0), \qquad w(t) = V(t,y_e(t)) \tag{67}$$

Furthermore,

$$y_e(t) = 2\sqrt{w(t)}, \tag{68}$$

which implies that

$$y_e(t) \leq e^{-c(r)(t-t_0)}y_e(t_0) \tag{69}$$

for all $t \geq t_0$, $|y_e(t_0)| \leq r$ and $r > 0$. Thus, we can conclude that the equilibrium point $y_e = 0$ is USGES (Definition 2.7. [21]).

We have thus proved that the cross track error dynamics (11) have global convergence to the equilibrium point $y_e = 0$. In addition, the local convergence properties are even stronger than asymptotic. In particular, it is shown that $y_e = 0$ is USGES and that the control objectives (12) are satisfied. □

VI. SIMULATION RESULTS

This section presents simulation results for two different curved paths. The simulated vehicle is a HUGIN AUV, produced by Kongsberg Maritime, restricted to movement in the horizontal plane. In all simulations, the desired relative surge velocity is chosen as $u_{\text{des}} = 3$ m/s and the lookahead distance Δ as $\Delta = 50$ m. The ocean current $\boldsymbol{V}_c = [0.3, 0.3]^T$ m/s, and the controller gains are chosen as $k_\psi = 1.2\text{s}^{-2}$, $k_r = 1.3\text{s}^{-1}$, $\lambda = 0.5\text{s}^{-1}$, $k_d = 0.1\text{s}^{-2}$, $k_u = 0.1\text{s}^{-1}$ and $k_e = 0.1\text{ms}^{-2}$. The dimensionless adaptive gains are chosen as $\gamma_u = \gamma_r = 0.1$. Note that to avoid chattering about the equilibrium point, in the simulations the discontinuous term $\text{sign}(z)$ in the controllers (19) and (21) has been replaced with the continuous function $\tanh(10z)$.

Two desired paths have been defined and simulated:

$$C_1 := \begin{cases} x_p(\theta) = & \theta \\ y_p(\theta) = & 30\sin(0.005\theta) \end{cases} \tag{70}$$

$$C_2 := \begin{cases} x_p(\theta) = & 1.2\theta\sin(0.005\theta) \\ y_p(\theta) = & 600\cos(0.005\theta) - 650 \end{cases} \tag{71}$$

Simulations results for the two paths are presented in Fig. 2-3 and 4-5, respectively. In both simulations, the cross-track error converges to zero and the relative surge velocity to the constant desired value. Thus, the control objectives are satisfied, and the controllers achieve tracking of the references ψ_{des} and $\dot{\psi}_{\text{des}}$.

Fig. 2 and 4 both illustrate that the USV side-slips to follow the desired path. The AUV heading is not aligned with the path heading, but the AUV velocity is aligned with the path, ensuring that the vessel follows the curved path without knowledge of the ocean current direction or magnitude.

VII. CONCLUSIONS

In this paper a guidance and control system for underactuated surface vessels is developed to solve the control objective of making the vessel follow a curved path in the presence of unknown ocean currents. The results are also applicable to AUVs moving in the horizontal plane.

The paper is motivated by the guidance law suggested in [14] designed for curved path following when no ocean currents are considered. We prove that a similar guidance law combined with an adaptive feedback linearizing controller with sliding mode, achieves convergence to the desired path with UGAS and USGES stability properties under explicit conditions. Only absolute velocity measurement are required. Simulation results verify the theoretical results.

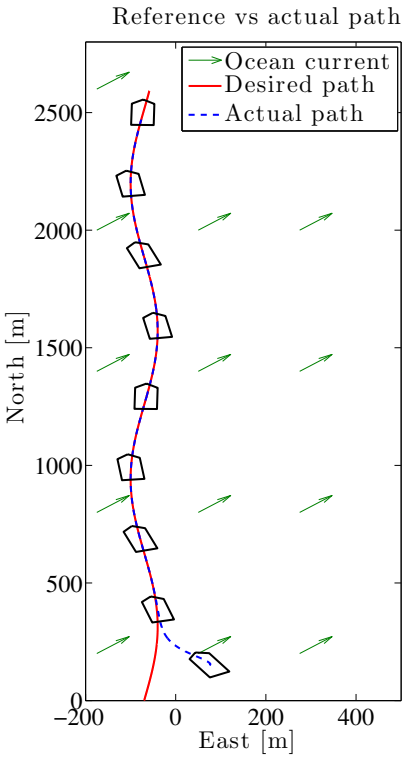

Fig. 2: Desired and actual path C_1.

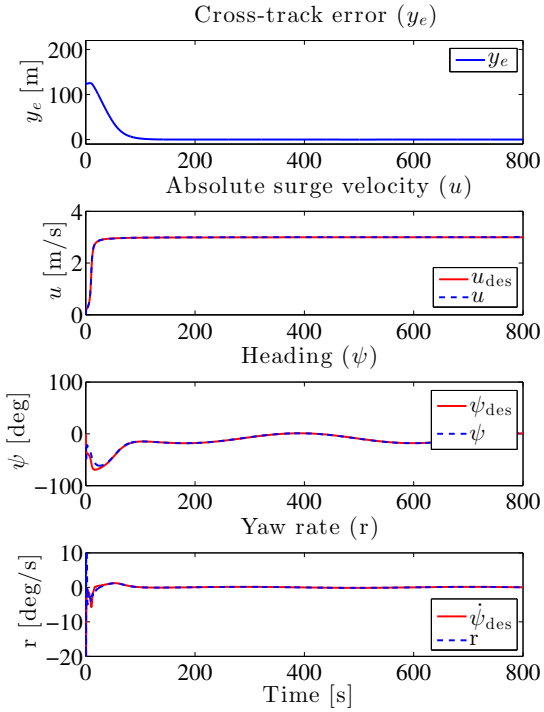

Fig. 3: Cross-track error and desired vs. actual surge velocity, yaw and yaw rate for C_1.

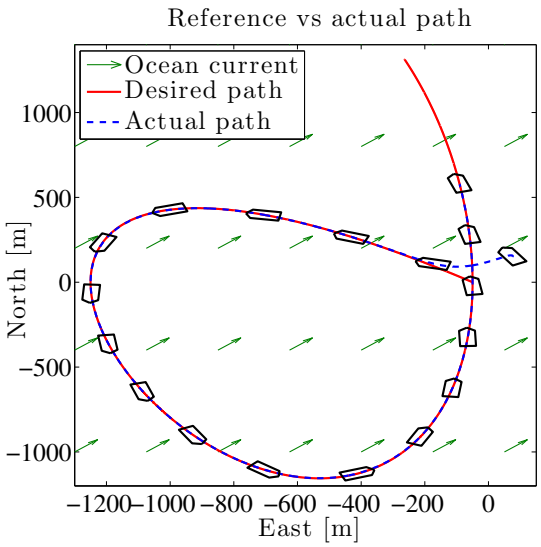

Fig. 4: Desired and actual path C_2.

APPENDIX A

$$\boldsymbol{\phi}_u(\psi,r) = \begin{bmatrix} \frac{d_{11}+2d_{11}^q u}{m_{11}}\cos(\psi) - \frac{m_{11}^A - m_{22}^A}{m_{11}} r\sin(\psi) \\ \frac{d_{11}+2d_{11}^q u}{m_{11}}\sin(\psi) + \frac{m_{11}^A - m_{22}^A}{m_{11}} r\cos(\psi) \\ -d_{11}^q\cos^2(\psi) \\ -d_{11}^q\sin^2(\psi) \\ -2d_{11}^q\cos(\psi)\sin(\psi) \end{bmatrix} \tag{72}$$

$$X(u_r,u_c) = \frac{1}{\Gamma}\Big(m_{33}(-d_{23} - m_{11}u_r - m_{11}^{RB}u_c) + m_{23}d_{33} + m_{23}(m_{23}u_r + m_{23}^{RB}u_c + m_{22}^A u_c)\Big) \tag{73}$$

$$Y(u_r) = \frac{1}{\Gamma}\Big(-m_{33}d_{22} + m_{23}d_{32} + m_{23}(m_{22}^A - m_{11}^A u_r)\Big) \tag{74}$$

$$F_r(u,v,r) = \frac{m_{22}}{\Gamma}\left(-(m_{22}v - m_{23}r)u + m_{11}uv - d_{32}v - d_{33}r\right) - \frac{m_{23}}{\Gamma}\left(-m_{11}ur - d_{22}v - d_{23}r\right) \tag{75}$$

Here, $\Gamma = m_{22}m_{33} - m_{23}^2 > 0$. Furthermore, the function $\boldsymbol{\phi}_r(u,v,r,\psi) = [\phi_{r1},\ldots,\phi_{r5}]^T$ is defined by

$$\begin{bmatrix}\phi_{r1}\\ \phi_{r2}\end{bmatrix} = \begin{bmatrix}\cos(\psi) & -\sin(\psi)\\ \sin(\psi) & \cos(\psi)\end{bmatrix}\begin{bmatrix}a_1\\ a_2\end{bmatrix} \tag{76}$$

$$\phi_{r3} = -\frac{m_{22}}{\Gamma}(m_{11}^A - m_{22}^A)\sin(\psi)\cos(\psi) \tag{77}$$

$$\phi_{r4} = \frac{m_{22}}{\Gamma}(m_{11}^A - m_{22}^A)\sin(\psi)\cos(\psi) \tag{78}$$

$$\phi_{r5} = \frac{m_{22}}{\Gamma}(m_{11}^A - m_{22}^A)(1 - 2\sin^2(\psi)), \tag{79}$$

where

$$a_1 = -\frac{m_{22}}{\Gamma}\Big((m_{11}^A - m_{22}^A)v + (m_{23}^A - m_{22}^A)r\Big) - \frac{m_{23}}{\Gamma}m_{11}^A r \tag{80}$$

$$a_2 = \frac{m_{22}}{\Gamma}\Big(d_{32} - (m_{11}^A - m_{22}^A)u\Big) - \frac{m_{23}}{\Gamma}d_{22} \tag{81}$$

Remark 5. In deriving the expression (74), we have used that $m_{11}^{RB} - m_{22}^{RB} = 0$, which follows from the fact that $m_{11}^{RB} = m_{22}^{RB} = m$, where m is the mass of the vessel [1].

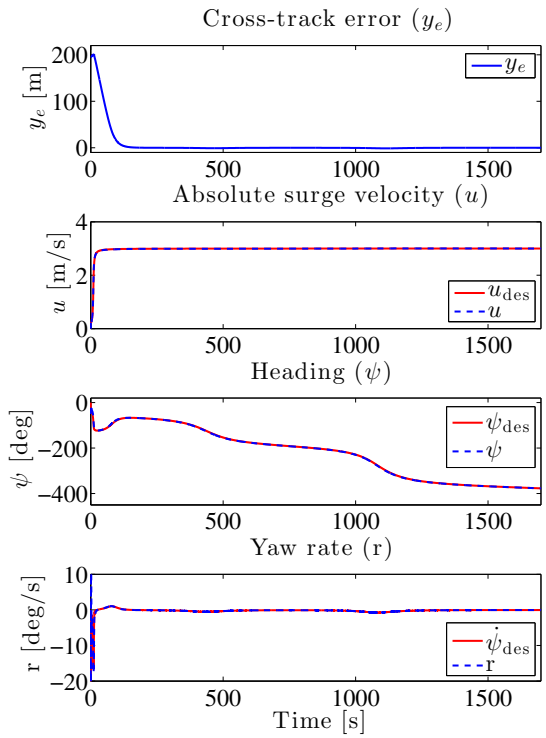

Fig. 5: Cross-track error and desired vs. actual surge velocity, yaw and yaw rate for C_2.

ACKNOWLEDGMENTS

This work was supported by the Research Council of Norway through the Center of Excellence funding scheme, project number 223254.

REFERENCES

[1] T. I. Fossen, *Handbook of Marine Craft Hydrodynamics and Motion Control*. Wiley, 2011.

[2] A. P. Aguiar and J. P. Hespanha, "Trajectory-Tracking and Path-Following of Underactuated Autonomous Vehicles With Parametric Modeling Uncertainty," *IEEE Transactions on Automatic Control*, vol. 52, no. 8, pp. 1362–1379, 2007.

[3] P. Encarnacao and A. Pascoal, "Combined trajectory tracking and path following: an application to the coordinated control of autonomous marine craft," in *Proc. 40th IEEE Conference on Decision and Control*, vol. 1, 2001, pp. 964–969.

[4] R. Skjetne, T. I. Fossen, and P. V. Kokotović, "Robust output maneuvering for a class of nonlinear systems," *Automatica*, vol. 40, no. 3, pp. 373–383, Mar. 2004.

[5] A. J. Healey and D. Lienard, "Multivariable sliding mode control for autonomous diving and steering of unmanned underwater vehicles," *IEEE Journal of Oceanic Engineering*, vol. 18, no. 3, pp. 327–339, 1993.

[6] A. M. Lekkas and T. I. Fossen, "Minimization of Cross-track and Along-track Errors for Path Tracking of Marine Underactuated Vehicles," in *Proc. European Control Conference*, 2014, pp. 3004–3010.

[7] ——, "Trajectory tracking and ocean current estimation for marine underactuated vehicles," in *Proc. 2014 IEEE Conference on Control Applications*. IEEE, Oct. 2014, pp. 905–910.

[8] R. Skjetne, U. Jorgensen, and A. R. Teel, "Line-of-sight path-following along regularly parametrized curves solved as a generic maneuvering problem," in *Proc. IEEE Conference on Decision and Control and European Control Conference*, 2011, pp. 2467–2474.

[9] P. Encarnacao, A. M. Pascoal, and M. Arcak, "Path Following for Marine Vehicles in the Presence of Unknown Currents," *Proc. 6th IFAC International Symposium on Robot Control*, pp. 469–474, 2000.

[10] K. Y. Pettersen and E. Lefeber, "Way-point tracking control of ships," in *Proc. IEEE Conference on Decision and Control*, vol. 1, 2001, pp. 940–945.

[11] E. Borhaug, A. Pavlov, and K. Y. Pettersen, "Integral LOS control for path following of underactuated marine surface vessels in the presence of constant ocean currents," in *Proc. 47th IEEE Conference on Decision and Control*, 2008, pp. 4984–4991.

[12] W. Caharija, M. Candeloro, K. Y. Pettersen, and A. J. Sorensen, "Relative Velocity Control and Integral LOS for Path Following of Underactuated Surface Vessels," *Proc. 9th IFAC Conference on Manoeuvring and Control of Marine Craft*, pp. 380–385, Sept. 2012.

[13] W. Caharija, K. Y. Pettersen, J. T. Gravdahl, and E. Borhaug, "Path following of underactuated autonomous underwater vehicles in the presence of ocean currents," in *Proc. 51st IEEE Conference on Decision and Control*, 2012, pp. 528–535.

[14] T. I. Fossen and K. Y. Pettersen, "On uniform semiglobal exponential stability (USGES) of proportional line-of-sight guidance laws," *Automatica*, vol. 50, no. 11, pp. 2912–2917, Nov. 2014.

[15] E. Borhaug and K. Y. Pettersen, "LOS path following for underactuated underwater vehicle," in *Proc. 7th IFAC Conference on Manoeuvring and Control of Marine Craft*, 2006.

[16] T. I. Fossen and A. M. Lekkas, "Direct and indirect adaptive integral line-of-sight path-following controllers for marine craft exposed to ocean currents," *International Journal of Adaptive Control and Signal Processing*, 2015.

[17] S. Moe, W. Caharija, K. Y. Pettersen, and I. Schjolberg, "Path following of underactuated marine surface vessels in the presence of unknown ocean currents," in *Proc. American Control Conference*, Portland, OR, USA, 2014, pp. 3856–3861.

[18] ——, "Path Following of Underactuated Marine Underwater Vehicles in the Presence of Unknown Ocean Currents," in *Proc. 33rd International Conference on Offshore Mechanics and Arctic Engineering*, vol. 7 - Ocean, San Francisco, CA, USA, 2014.

[19] A. Loria, E. Panteley, D. Popovic, and A. R. Teel, "A nested Matrosov theorem and persistency of excitation for uniform convergence in stable nonautonomous systems," *IEEE Transactions on Automatic Control*, vol. 50, no. 2, pp. 183–198, Feb. 2005.

[20] H. K. Khalil, *Nonlinear systems*. Prentice Hall PTR, 2002.

[21] A. Loria and E. Panteley, *Advanced Topics in Control Systems Theory: Lecture Notes from FAP 2004*. London: Springer, 2004, ch. 2: Cascaded Nonlinear Time-Varying Systems: Analysis and Design, pp. 23–64.